

## Some Problems on the Analysis of the Earth Tides

Takeshi MIKUMO

*Disaster Prevention Research Institute, Kyoto University*

and

Ichiro NAKAGAWA

*Geophysical Institute, Faculty of Science, Kyoto University*

### Abstract

The spectral structure of the earth tides which have been observed during one year by an Askania gravimeter at Kyoto, and that of the corresponding theoretical tides on a rigid earth, were compared to determine the tidal factor of gravity and the phase lag with a high precision. A band-pass filter that has dominant responses only for semidiurnal or diurnal frequencies was applied to both of the tidal functions, to eliminate the effects of drift and of contamination from other constituents. Variations in the two tidal parameters during the period were also examined, extracting only  $M_2$  or  $O_1$  wave by the use of a narrow Gaussian filter. These results show long-period fluctuations with several months, suggesting a limit for discussions on elastic and anelastic behavior of the earth.

### §1. Introduction

For the analysis of the earth tides various methods have so far been developed, making significant contributions to the evaluation of overall elastic properties of the earth. It is noticed, however, that there have been rather scattered estimates for the tidal factor of gravity and the phase lag. The reason for this may be attributed partly to the effects of oceanic tides, atmospheric pressure and temperature variations or to local crustal structure, but it appears that some of the scattering arise from the methodological difference in the time length of analysis, the elimination of drift and the treatment of theoretical tides to be compared with observations.

Our main purpose in the present paper will be focused to determine, with a high precision, the tidal factor of gravity  $G$  and particularly the phase lag  $\kappa$  from more complete analyses for reducing the above effects to a minimum extent, in order to test a future possibility of evaluating anelasticity of the whole earth from observations of the earth tides.

For this purpose, the following analyses are made by applying the Fourier transform

and digital filtering techniques both to an observed record and to the corresponding theoretical tides. (1) The spectral structure of the observed tides and that predicted theoretically for a perfectly rigid earth are compared, and the two tidal parameters,  $G$ , and  $\kappa$ , for major constituents are then determined. (2) To eliminate the effects of drift and of contamination from other constituents, a band-pass filter which has dominant responses for semidiurnal or diurnal frequencies is applied to the observed and theoretical tides prior to the Fourier analysis. (3) A specific constituent ( $M_2$  or  $O_1$ ) is extracted from the observed and theoretical tides using a narrow Gaussian filter, and the filtered functions are Fourier-analysed over successive time ranges with an appropriate length to examine possible time variations in  $G$  and  $\kappa$ .

### §2. Observed and Theoretical Tides

Data analysed are the earth tides record that has been obtained by the Askania gravimeter Gs-11 (No. 111) at the Geophysical Institute of Kyoto University (35°02' N, 135°47' E,  $h=60$  m) during one year from August 1, 00 h 00 m, 1959 to July 31, 23 h 00 m, 1960 (NAKAGAWA, 1962). A total of 8,784 hourly

values were digitized from the record.

In some conventional methods of tidal analysis, theoretical amplitudes of each tidal constituent are derived from the mean position of the tide-generating bodies, or with some corrections, but they do not correspond exactly to the amplitudes over a specific observation period. For a more appropriate comparison with observations, theoretical tidal variation of gravity based on a perfectly rigid earth has been computed here, for the same period and time intervals as the above observation, from some modification of LONGMAN's formulae (1959) referring to BARTEL's (1957).

Both the observed and theoretical tides are then analysed by the same methods described below.

### § 3. Spectral Structure

The spectrum of the earth tides may be obtained by the conventional Fourier transform,

$$F(\omega) = \frac{1}{T} \int_{-T}^T f(t) e^{-i\omega t} dt \quad (1)$$

where  $f(t)$  is the observed or theoretical tidal function and  $2T$  is the time interval of analysis.  $F(\omega)$  is actually the spectrum of a truncated function, which is zero outside the interval  $|t| \leq T$ . The truncation will cause contamination of the spectrum by energy leakage particularly in the vicinity of strong spectral peaks. Applying the Hanning data window

$$D(t) = \begin{cases} \frac{1}{2} \left( 1 + \cos \frac{\pi t}{T} \right) & \text{for } |t| \leq T \\ 0 & \text{for } |t| > T \end{cases} \quad (2)$$

to  $f(t)$ , to reduce the effects of contamination, we have

$$\begin{aligned} g(t) &= D(t) \cdot f(t) \\ &= \frac{1}{2} f(t) + \frac{1}{4} f(t) e^{i\omega_0 t/2} + \frac{1}{4} f(t) e^{-i\omega_0 t/2} \end{aligned} \quad \left. \begin{array}{l} \\ \\ \end{array} \right\} \quad (3)$$

Therefore,

$$G(\omega) = \frac{1}{2} F(\omega) + \frac{1}{4} F\left(\omega + \frac{\omega_0}{2}\right) + \frac{1}{4} F\left(\omega - \frac{\omega_0}{2}\right)$$

The spectrum  $F(\omega)$  for the observed tides

has been computed in a previous paper (NAKAGAWA, MIKUMO and TANAKA, 1966) after removing a linear term of drift, so that the smoothed spectrum  $G(\omega)$  can be obtained by the above procedure. The corresponding spectrum of the theoretical tides has also been computed here, using the same technique. Figs. 1 and 2 show the spectral structure of the observed and theoretical tides over semidiurnal and diurnal frequency ranges respectively. Although the application of the data window broadens the side lobe of each spectral peak and reduces its amplitude to about a half, the ordinate indicates the absolute amplitude, which has been corrected by multiplying a constant to recover the original amplitude for major constituents. The features of the observed amplitude spectrum are in close agreement with those of the theoretical spectrum, as have been demonstrated in some previous work (JOBERT, 1963a; BARSENKOV, 1967), except the absolute amplitudes, which are a function of the location of an observation station. It can be seen that spectral peaks occur for  $M_2$ ,  $S_2$ ,  $N_2$ ,  $K_2$  and  $L_2$  in a semidiurnal frequency range and for  $K_1$ ,  $O_1$ ,  $P_1$ ,  $Q_1$  and  $M_1$  in a diurnal range.

The tidal factor  $G$  and the phase lag  $\kappa$  were calculated from the amplitude and phase spectrums for the frequency appropriate to each constituent, as in the earlier work of this kind (HARRISON *et al.*, 1963; SLICHTER *et al.*, 1964),

$$G = A_0/A_T \text{ and } \kappa = \varphi_0 - \varphi_T \quad (4)$$

The results are given in the upper half of Table 1. The determined amplitudes and phases differ somewhat from those given in the previous paper, since the previous results have been corrected for the location of the moon and the sun to the central epoch of the observation.

### § 4. Effects of the Drift and Other Tidal Constituents

In the usual harmonic analysis, the instrumental drift involved in observed records had been eliminated by various methods such as Pertzev's or some other combinations of

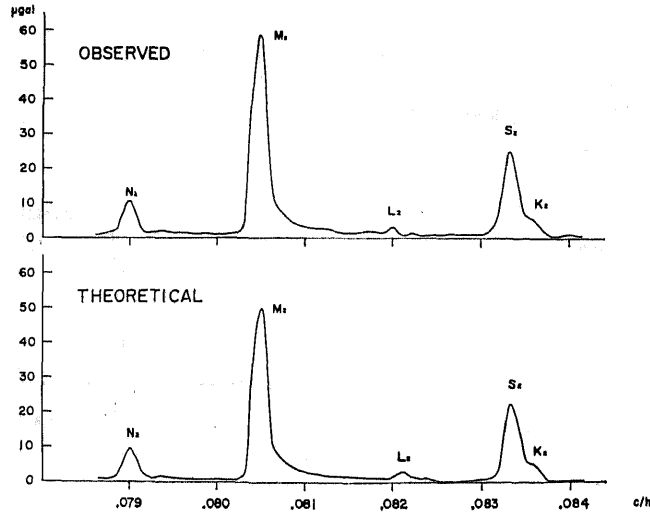


Fig. 1. Spectral structure over semidiurnal frequencies.

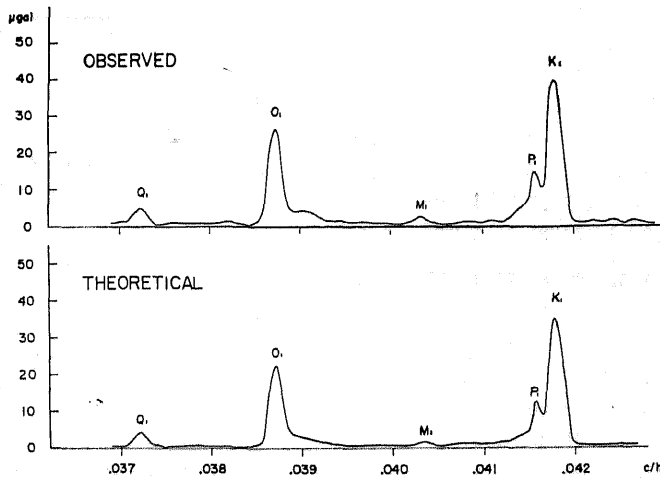


Fig. 2. Spectral structure over diurnal frequencies.

ordinates, but it does not appear that some of them have a sufficient precision for the present purpose.

An alternative technique is presented here to use a band-pass filter similar to that designed by JOBERT (1963b) and TANAKA and MIKUMO (1965), which has dominant responses only for semidiurnal or diurnal frequencies, rejecting all other frequencies as noises. Let the frequency response of the filter be  $A(\omega)$  for  $\omega_1 < \omega < \omega_2$  and otherwise zero, then its impulse response  $h(t)$  is,

$$h(t) = \frac{1}{2\pi} \int_{\omega_1}^{\omega_2} A(\omega) \cos \omega t \, d\omega \quad (5)$$

which, if the interval  $[\omega_1, \omega_2]$  is divided into

$n$  subintervals  $[\omega_j - \Delta\omega_j/2, \omega_j + \Delta\omega_j/2]$ , may be approximated by,

$$\cong \frac{1}{\pi} \sum_{j=1}^n \left[ A(\omega_j) \Delta\omega_j \frac{\sin \varphi}{\varphi} \cos \omega_j t - \left( \frac{\partial A}{\partial \omega} \right)_j \Delta\omega_j \left( \frac{\sin \varphi}{\varphi} - \cos \varphi \right) \frac{\sin \omega_j t}{t} \right] \quad (6)$$

where

$$\varphi = \Delta\omega_j t / 2.$$

The filtered tides  $\bar{f}(t)$  will be obtained by convolving the original tide function  $f(t)$  with  $h(t)$ ,

$$\bar{f}(t) = \int_{-\tau_1}^{\tau_1} f(t-\tau) h(\tau) \, d\tau \quad (7)$$

The limited length of the impulse response

Table 1. Results of analysis.

$A_0$ ; amplitude of observed tides,  $A_T$ ; amplitude of theoretical tides

$\varphi_0$ ; phase of observed tides,  $\varphi_T$ ; phase of theoretical tides

$G$ ; tidal factor defined by  $G=A_0/A_T$

$\kappa$ ; phase lag defined by  $\kappa=\varphi_0-\varphi_T$

(1) results from unfiltered tides over the period:  
August 1, 00 h 00 m, 1959—July 31, 23 h 00 m, 1960 (8784 hours)

(2) results from band-pass filtered tides over the period:  
August 31, 00 h 00 m, 1959—June 25, 23 h 00 m, 1960 (7344 hours)

	Observed		Theoretical		$G$	$\kappa$	
	$A_0$	$\varphi_0$	$A_T$	$\varphi_T$			
	$\mu$ gal	deg.	$\mu$ gal	deg.		deg.	
(1)	$M_2$	60.535	170.02	52.243	172.00	1.160	-1.98
	$S_2$	25.535	96.31	23.337	90.79	1.095	5.52
	$N_2$	10.504	312.49	9.874	315.89	1.064	-3.40
	$K_2$	5.727	353.99	5.028	353.24	1.140	0.75
	$K_1$	40.992	171.99	36.152	173.87	1.134	-1.88
	$O_1$	27.284	178.90	23.590	178.67	1.156	0.23
	$P_1$	15.136	94.47	13.532	95.38	1.120	-0.91
	$Q_1$	5.644	320.34	4.477	321.81	1.260	-1.47
(2)	$M_2$	60.418	158.55	52.307	160.54	1.155	-1.99
	$S_2$	26.179	97.48	23.843	92.03	1.098	5.45
	$N_2$	10.635	270.70	10.078	273.86	1.055	-3.16
	$K_2$	7.677	25.62	6.689	21.41	1.147	4.21
	$K_1$	40.790	203.33	35.775	206.74	1.140	-3.41
	$O_1$	27.355	138.26	23.561	137.84	1.161	0.42
	$P_1$	16.040	41.72	13.746	41.15	1.167	0.57
	$Q_1$	6.001	253.73	4.859	251.80	1.235	1.93

gives a slight distortion to the designed filter, but a sufficiently long duration ( $2\tau_1=1440$  hours) has reduced the distortion to a negligible extent, as may be seen in Figs. 3 and 4. The amplitude and phase of specific constituents filtered from the observed and theoretical tides were determined again by the Fourier transform in the same way as in equation (1), and the results obtained are shown in the lower half of Table 1. A comparison of the presented results with those from the unfiltered tides shows that the discrepancies in  $G$  and  $\kappa$  are less than 0.5% and  $0.2^\circ$  respectively in both cases of  $M_2$  and

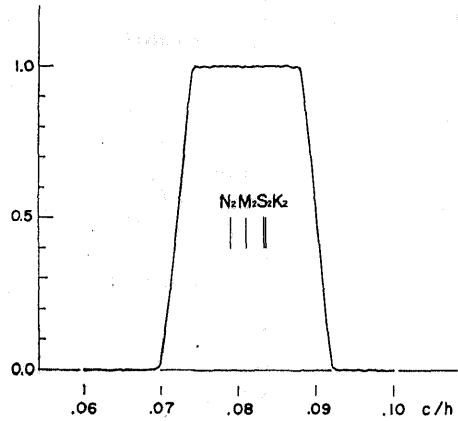


Fig. 3. Band-pass filter for semidiurnal frequencies.

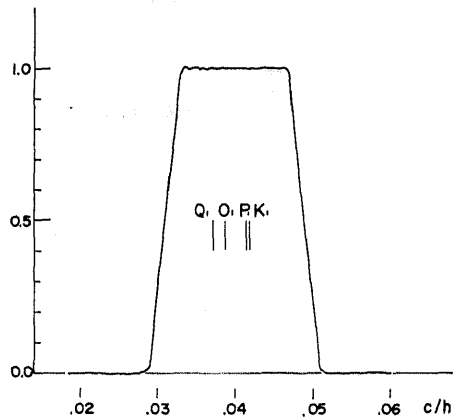


Fig. 4. Band-pass filter for diurnal frequencies.

$O_1$ . The implication of the discrepancies is that, as far as we use the Fourier transform to determine the tidal parameters, the effects of the drift and of contamination from other constituents may be regarded as insignificant, as would be expected theoretically. The slight discrepancies may be due to shortening of the analysed time interval by two months in the filtered tides. The application of digital filtering of this kind may also be useful for the case with a more complex pattern of drift.

§ 5. Variations in the Tidal Factor and the Phase Lag

Another problem is to extract a specific constituent from the observed or theoretical tides by the use of a sharper filter like Gaus-

sian's, for the purpose of examining whether significant variations in the tidal factor  $G$  and the phase lag  $\kappa$  exist during an observation period. The response of the Gaussian filter in the frequency domain is

$$A(\omega) = e^{-\alpha(\omega - \omega_0)^2} \quad (8)$$

Its impulse response is expressed as

$$h(t) = \frac{1}{2\sqrt{\pi\alpha}} \exp(-t^2/4\alpha) \cos \omega_0 t \quad (9)$$

where  $\alpha$  is a constant which specifies a sharpness of the filter, and  $\omega_0$  is the angular frequency which gives a maximum of  $A(\omega)$ . Figs. 5 and 6 show the Gaussian filter used

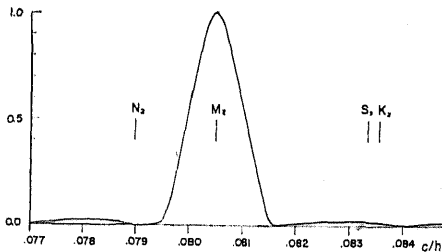


Fig. 5. Gaussian filter for  $M_2$ .

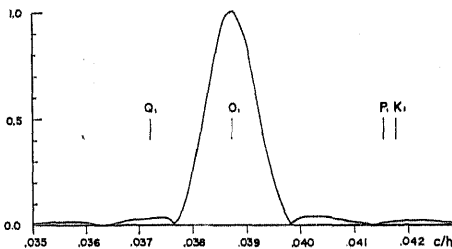


Fig. 6. Gaussian filter for  $O_1$ .

for  $M_2$  and  $O_1$  constituents, respectively. Small undulations at the wings result from a limited length of the impulse response. If the impulse response is convolved with the observed or theoretical tide function following equation (7), the filtered function  $\bar{f}(t)$  consists mostly of a sinusoidal wave with an angular frequency of  $\omega_0$ . We tentatively divide the function over a length of 10 months into twenty time intervals, each having 15 days' period. The Fourier transform yields the amplitude and phase of  $M_2$  or  $O_1$  constituent for each of the divided intervals from the observed and theoretical tides res-

pectively. In Table 2, thus determined values are tabulated. It is noted that the variation in the theoretical amplitudes over twenty intervals does not exceed 0.3% in the case of  $M_2$  and 0.8% for  $O_1$ . This suggests that the amplitude of the constituent  $M_2$  may be determined to a precision of about 0.3% from 15 days' filtered record and that time variations in the tidal factor exceeding the limit, if they exist, could be detected by the combined use of a sharp filter and the Fourier analysis.

The observed amplitudes indicate, however, variations as large as 2.5% in the case of  $M_2$ , and hence yield the same order of variation in  $G$ . The  $O_1$  constituent shows much larger variations in the observed amplitudes and the tidal factor. The variations in  $G$  and  $\kappa$  are shown in Figs. 7 and 8. The vertical lines at the middle of each analysed interval indicate a possible range of the errors estimated from the accuracy of calibration for the gravimeter used. (NAKAGAWA, 1962). The tidal factor of  $M_2$  is found to be between 1.13 and 1.18 and the corresponding phase lag ranges from  $-0.6^\circ$  to  $-3.8^\circ$ . It may also be noticed from the two figures that there is a long-period fluctuation of about four months both in  $G$  and  $\kappa$ , and that the fluctuation of  $G$  is not in phase with that of  $\kappa$ .

## §7. Discussion and Concluding Remarks

Previous results (NAKAGAWA, 1962) for the same observation, which were obtained by Lecolazet's method, have yielded variations with higher frequencies in the two parameters both for  $M_2$  and  $O_1$ . In some analyses using Lecolazet's or Pertzov's method, shorter-period fluctuations of  $G$  with the order of several hours or several days have been described and interpreted as random observational errors (SARITSCEVA, 1964; KRAMER, 1964). It appears that long-period fluctuations that may be compared with the present case have been noted only in a long term observation (PARIISKII *et al.*, 1967). It would be difficult, however, to attribute these fluctuations to any definite sources such as er-

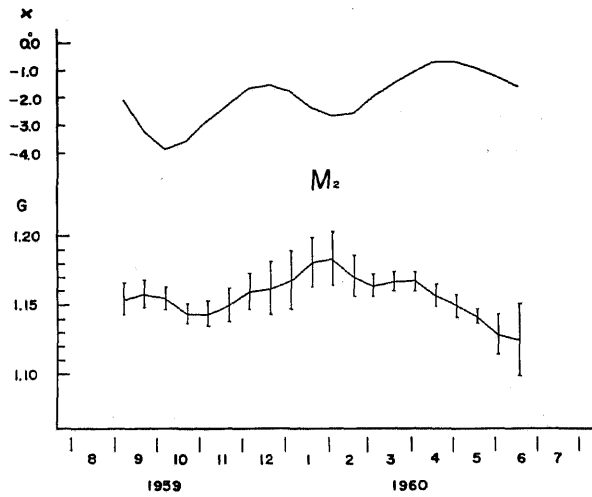


Fig. 7. Variations in  $G$  and  $\kappa$  of  $M_2$  over every 15 days.

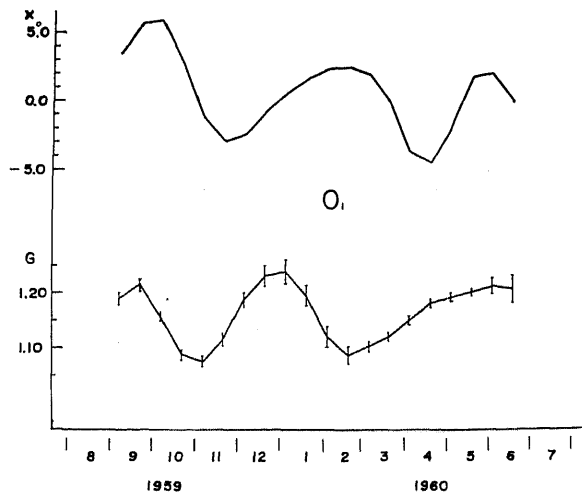


Fig. 8. Variations in  $G$  and  $\kappa$  of  $Q_1$  over every 15 days.

rors in the instrumental calibration or drift, since the effects have been estimated or removed already.

To examine the effect of the time length of analysis and a possible correlation of the fluctuations with the amplitudes of the observed tides, similar analyses have been made of  $M_2$  for four different time intervals; *a*) between two successive times for the full moon, *b*) the times for the new moon, *c*) the time from the full moon to the new moon, and *d*) between the time from the new moon to the full moon. The former two

cases (a) and (b) correspond to a synodical month, which was taken to be 708 hours in the present analysis, while 354 hours were taken for the latter two cases (c) and (d). The tidal factor and the phase lag thus obtained are shown in Table 3 and plotted in Fig. 9 by different symbols. No significant differences can be recognized among the parameters determined for the four time intervals, and the variations in  $G$  and  $\kappa$  agree also with the foregoing results (Fig. 7).

There leaves a possibility that seasonal variations in the effects of oceanic tides and

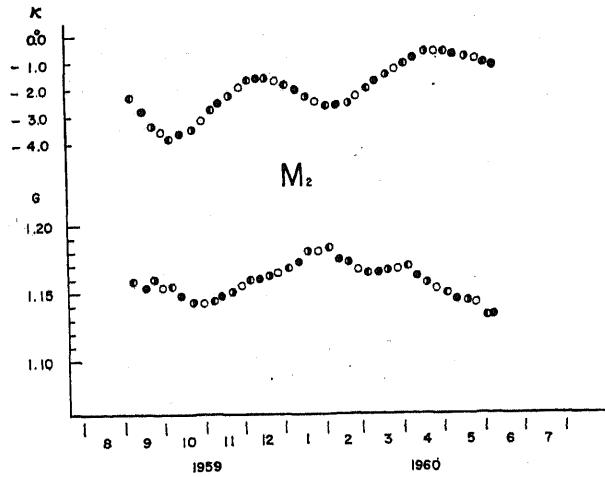


Fig. 9. Variations in  $G$  and  $\kappa$  of  $M_2$  from the analysis for four different time intervals.

○; full moon—full moon ●; new moon—new moon  
◐; full moon—new moon ◑; new moon—full moon

Table 2. Variations in the tidal parameters of  $M_2$  and  $O_1$  over every 15 days' period.

No.	Period	$M_2$						$O_1$					
		$A_0$	$\varphi_0$	$A_T$	$\varphi_T$	$G$	$\kappa$	$A_0$	$\varphi_0$	$A_T$	$\varphi_T$	$G$	$\kappa$
		$\mu\text{gal}$	deg.	$\mu\text{gal}$	deg.		deg.	$\mu\text{gal}$	deg.	$\mu\text{gal}$	deg.		deg.
1	1959 Aug. 31—Sept. 14	60.374	158.47	52.315	160.58	1.154	-2.11	28.363	138.06	23.849	134.59	1.189	3.47
2	Sept. 15—Sept. 29	60.533	151.50	52.266	154.75	1.158	-3.25	28.994	120.03	23.835	114.30	1.216	5.73
3	Sept. 30—Oct. 14	60.376	145.21	52.251	149.05	1.155	-3.84	27.529	100.04	23.821	94.13	1.156	5.91
4	Oct. 15—Oct. 29	59.693	139.66	52.199	143.23	1.144	-3.57	25.785	76.71	23.753	73.87	1.086	2.84
5	Oct. 30—Nov. 13	59.705	134.70	52.167	137.53	1.144	-2.83	25.475	52.42	23.718	53.58	1.074	-1.16
6	Nov. 14—Nov. 28	60.075	129.44	52.150	131.72	1.150	-2.28	26.364	23.25	30.647	33.17	1.115	-2.92
7	Nov. 29—Dec. 13	60.470	124.32	52.135	126.02	1.160	-1.70	28.103	10.35	23.676	12.83	1.187	-2.48
8	Dec. 14—Dec. 28	60.640	118.65	52.180	120.22	1.162	-1.57	29.174	351.62	23.710	352.35	1.230	-0.73
9	Dec. 29—Jan. 12	60.960	112.70	52.201	114.50	1.168	-1.80	29.470	332.81	23.781	332.15	1.239	0.66
10	1960 Jan. 13—Jan. 27	61.766	106.40	52.291	108.72	1.181	-2.32	28.516	313.62	23.891	311.86	1.194	1.76
11	Jan. 28—Feb. 11	61.912	100.33	52.321	103.00	1.183	-2.67	26.740	294.25	23.900	291.77	1.119	2.48
12	Feb. 12—Feb. 26	61.358	94.66	52.414	97.23	1.171	-2.57	25.972	274.19	23.937	271.62	1.085	2.57
13	Feb. 27—Mar. 12	61.012	89.53	52.408	91.50	1.164	-1.97	26.269	253.44	23.859	251.40	1.101	2.04
14	Mar. 13—Mar. 27	61.218	84.26	52.463	85.76	1.167	-1.50	26.661	230.18	23.820	231.06	1.119	-0.88
15	Mar. 28—Apr. 11	61.211	78.99	52.401	80.02	1.168	-1.03	27.313	206.05	23.747	210.62	1.150	-4.57
16	Apr. 12—Apr. 26	60.611	73.66	52.401	74.29	1.157	-0.63	28.108	184.87	23.782	190.10	1.182	-5.23
17	Apr. 27—May 11	60.148	67.89	52.305	68.54	1.150	-0.65	28.406	167.86	23.790	169.63	1.194	-1.77
18	May 12—May 26	59.676	61.98	52.278	62.82	1.142	-0.84	28.760	151.35	23.916	149.33	1.203	2.02
19	May 27—June 10	58.934	55.93	52.193	57.05	1.129	-1.12	29.091	131.43	23.969	129.05	1.214	2.38
20	June 11—June 25	58.707	49.85	52.182	51.34	1.125	-1.49	29.056	109.35	24.028	109.07	1.209	0.28

in meteorological disturbances could contribute to the long-period fluctuation of the tidal parameters. However, the result that the phase of the fluctuation does not coincide between  $M_2$  and  $O_1$  and between  $G$  and  $\kappa$  introduces difficulty into the interpretation.

Table 3. Variations in the tidal parameters of  $M_2$  over every 708 hours (a) from full moon to full moon, and from new moon to new moon, (b) and over every 354 hours from full moon to new moon, and from new moon to full moon.

No.	Period		$A_0$	$\varphi_0$	$A_T$	$\varphi_T$	$G$	$\kappa$
			$\mu\text{gal}$	deg.	$\mu\text{gal}$	deg.		
(a)	1959	Sept. 2 06 h—Oct. 1 18 h	60.301	282.84	52.280	285.66	1.153	-2.82
		Sept. 17 00 h—Oct. 16 12 h	60.294	102.41	52.239	106.01	1.154	-3.60
		Oct. 1 18 h—Oct. 31 06 h	59.945	282.68	52.197	286.35	1.148	-3.67
		Oct. 16 12 h—Nov. 15 00 h	59.561	103.56	52.144	106.70	1.142	-3.14
		Oct. 31 06 h—Nov. 29 18 h	59.847	284.54	52.110	287.05	1.148	-2.51
		Nov. 15 00 h—Dec. 14 12 h	60.163	105.42	52.083	107.39	1.155	-1.97
		Nov. 29 18 h—Dec. 29 06 h	60.440	286.11	52.089	287.74	1.160	-1.63
		Dec. 14 12 h—Jan. 13 00 h	60.666	106.39	52.107	108.08	1.164	-1.69
		Dec. 29 06 h—Jan. 27 18 h	61.154	286.36	52.151	288.42	1.173	-2.06
	1960	Jan. 13 00 h—Feb. 11 12 h	61.612	106.27	52.196	108.76	1.180	-2.49
		Jan. 27 18 h—Feb. 26 06 h	61.399	286.48	52.244	289.11	1.175	-2.63
		Feb. 11 12 h—Mar. 12 00 h	60.992	107.13	52.277	109.44	1.167	-2.31
		Feb. 26 06 h—Mar. 26 18 h	60.920	288.02	52.295	289.79	1.165	-1.77
		Mar. 12 00 h—Apr. 10 12 h	61.025	108.82	52.290	110.12	1.167	-1.30
		Mar. 26 18 h—Apr. 25 00 h	60.740	289.61	52.259	290.47	1.162	-0.86
		Apr. 10 12 h—May 10 00 h	60.207	110.17	52.217	110.81	1.153	-0.64
		Apr. 25 00 h—May 24 18 h	59.743	290.45	52.159	291.16	1.145	-0.71
		May 10 00 h—June 8 12 h	59.007	110.57	52.111	111.51	1.132	-0.94
		May 24 18 h—June 23 06 h	58.524	290.61	52.065	291.85	1.124	-1.24
(b)	1959	Sept. 2 06 h—Sept. 17 00 h	60.644	283.39	52.389	285.67	1.158	-2.23
		Sept. 17 00 h—Oct. 1 18 h	60.675	102.62	52.317	105.98	1.160	-3.36
		Oct. 1 18 h—Oct. 16 12 h	60.425	282.53	52.307	286.37	1.155	-3.84
		Oct. 16 12 h—Oct. 31 06 h	59.693	103.15	52.232	106.66	1.143	-3.51
		Oct. 31 06 h—Nov. 15 00 h	59.695	284.29	52.199	287.06	1.144	-2.77
		Nov. 15 00 h—Nov. 29 18 h	60.039	105.10	52.162	107.36	1.151	-2.26
		Nov. 29 18 h—Dec. 14 12 h	60.470	286.07	52.145	287.75	1.160	-1.68
		Dec. 14 12 h—Dec. 29 06 h	60.629	106.48	52.173	108.05	1.162	-1.57
		Dec. 29 06 h—Jan. 13 00 h	60.940	286.62	52.183	288.43	1.168	-1.81
	1960	Jan. 13 00 h—Jan. 27 18 h	61.725	106.42	52.259	108.74	1.181	-2.32
		Jan. 27 18 h—Feb. 11 12 h	61.862	286.43	52.271	289.10	1.183	-2.67
		Feb. 11 12 h—Feb. 26 06 h	61.352	106.84	52.355	109.43	1.172	-2.59
		Feb. 26 06 h—Mar. 12 00 h	60.905	287.75	52.339	289.77	1.164	-2.02
		Mar. 12 00 h—Mar. 26 18 h	61.070	108.60	52.390	110.12	1.166	-1.52
		Mar. 26 18 h—Apr. 10 12 h	61.155	289.37	52.328	290.45	1.169	-1.08
		Apr. 10 12 h—Apr. 25 00 h	60.555	110.17	52.326	110.82	1.157	-0.65
		Apr. 25 00 h—May 10 00 h	60.089	290.50	52.245	291.12	1.150	-0.62
		May 10 00 h—May 24 18 h	59.732	110.72	52.210	111.52	1.144	-0.80
		May 24 18 h—June 8 12 h	59.105	290.74	52.149	291.81	1.133	-1.07



Detailed discussions on this problem require more observations covering a long period made concurrently at several stations with different kinds of gravimeters.

The rather large variations in the phase lag  $\kappa$  make it difficult to evaluate anelasticity of the whole earth following MACDONALD's method (1964), although the best determination is that for  $M_2$ , a mean phase lag of which being about  $-2^\circ.0$ . Further developments on this side would not be expected, until the instrumental phase delay can be well calibrated and the effects of oceanic tides and other disturbances could be removed by proper techniques.

### Acknowledgments

We wish to thank Drs. Michio Otsuka and Torao Tanaka for several comments on the manuscript, and Mrs. Ritsuko Koizumi for assistance in the analysis. Numerical computations were made on a HITAC 5020E at the Computation Center, University of Tokyo.

### References

- BARSENKOV, S. N.:  
1967, A spectral analysis of tidal variations in the force of gravity at Talgar, *Izv. Akad. Nauk, SSSR*, **3** (English Translation), 170-174.
- BARTELS, J.:  
1957, *Gezeitenkräfte*, Handbuch der Physik, XLVIII, Geophysik II, 747, Springer-Verlag, Berlin.
- HARRISON, J. C., N. F. NESS, I. M. LONGMAN, R. F. S. FORBES, E. A. KRAUT and L. B. SLICHTER:  
1963, Earth-tide observations made during the International Geophysical Year, *J. Geophys. Res.*, **68**, 1497-1516.
- JOBERT, G.:  
1963a, Comparaison des résultats de l'analyse spectrale des marées terrestres avec les résultats théoriques, *Marées Terrestres*, Bulletin d'Informations, **33**, 1013-1016.
- JOBERT, G.:  
1963b, Sur les filtres numériques utilisés dans l'analyse harmonique, *ibid.*, **33**, 1260-1273.
- KRAMER, M. V.:  
1964, On the effect of chance errors of observations upon the results of determination of amplitudes and phases of elastic tidal waves, *Communications Observatoire Royal de Belgique No. 236, Série Géophysique*, **69**, 426-437.
- LONGMAN, I. M.:  
1959, Formulas for computing the tidal accelerations due to the Moon and the Sun, *J. Geophys. Res.*, **64**, 2351-2355.
- MACDONALD, G. J. F.:  
1964, Tidal friction, *Rev. Geophys.*, **2**, 524-530.
- NAKAGAWA, I.:  
1962, Some problems on time change of gravity, Part 3, On precise observation of gravity at the Gravity Reference Station, *Bull. Disaster Prevention Res. Inst., Kyoto Univ.*, **57**, 2-65.
- NAKAGAWA, I., T. MIKUMO and T. TANAKA:  
1966, Spectral structure of the earth tides and related phenomena—gravimetric record—, *Spec. Contr. Geophys. Inst., Kyoto Univ.*, **6**, 215-223.
- PARIISKII, N. N., S. H. BARSENKOV, V. A. VOLKOV, D. G. GRIDNEV and M. V. KRAMER:  
1967, Results of 19 month observations of earth tides in Talgar, *Izv. Akad. Nauk, SSSR*, **10** (English Translation), 107-114.
- SARITSCEVA, J. K.:  
1964, Sur la dispersion des valeurs du facteur  $\delta$  obtenue par la méthode de R. Lecolazet pour la même station, *Communications Observatoire Royal de Belgique No. 236, Série Géophysique*, **69**, 421-425.
- SLICHTER, L. B., G. J. F. MACDONALD, M. CAPUTO and C. L. HAGER:  
1964, Report of earth tides results and of other gravity observations at UCLA, *ibid.*, 172-177.
- TANAKA, T. and T. MIKUMO:  
1965, An application of digital filtering to the record of ground deformation, *J. Seism. Soc. Japan, Series II*, **18**, 235-244.

(Received July 25, 1968)